FABAD J. Pharm. Sci., 43, 3, 249-261, 2018

RESEARCH ARTICLE

Synthesis, Molecular Docking and Antibacterial Activity Evaluation of some Novel 3,7-disubstituted-[1,3] thiazolo[4,5-d]pyrimidin-2(3*H*)-one Derivatives

Unni JAYARAM[*,º], Mohammed AFZAL AZAM[*], Raman RAJESHKUMAR[**]

Synthesis, Molecular Docking and Antibacterial Activity Evaluation of some Novel 3,7-disubstituted-[1,3] thiazolo[4,5-d]pyrimidin-2(3H)-one Derivatives

SUMMARY

In the present study we synthesized novel 3,7-disubstituted-[1,3] thiazolo[4,5-d]pyrimidin-2(3H)-ones (2a, 3a, 4a and 4b) and characterized them by spectral data. Synthesized compounds were evaluated for their antibacterial activity against selected strains of Gram-positive and Gram-negative bacteria by the disk diffusion and broth dilution methods. Some of the tested compounds exhibited promising activity against the tested bacterial strains. Among the tested compounds, 4a exhibited maximum inhibitory activity against Escherichia coli and Staphylococcus aureus with MIC values of 6.25 and 12.5 µg/ml, respectively. The molecular modeling studies for the synthesized compounds were performed to predict the binding mode of these compounds within the active site of E. coli DNA Gyrase (GyrB) and DNA Topoisomerase IV (ParE) subunits. Further, their ADMET properties are computed

Key Words: *Thiazolopyrimidines, antibacterial activity, docking, GyraseB, ParE, synthesis.*

Bazı Yeni 3,7-disübstitüe- [1,3] tiyazolo[4,5-d]pirimidin-2(3H)-on Türevlerinin Sentezi, Moleküler Docking Çalışmaları ve Antibakteriyel Aktivitelerinin Değerlendirmesi

ÖZET

Bu çalışmada yeni 3,7-disübstitüe-[1,3] tiyazolo[4,5-d]pirimidin-2(3H)-on türevi bileşikler sentezlenmiş (2a, 3a, 4a ve 4b) ve bu bileşiklerin yapıları spektral verilerle tanımlanmıştır. Sentezlenen bileşiklerin antibakteriyel aktivitesi; gram pozitif ve gram negatif bakteri suşlarına karşı disk difüzyon ve tüp (broth) dilüsyon metodu ile tayin edilmiştir.Test edilen bileşiklerin bazıları test edilen bakteriyel suşlara karşı güçlü aktivite göstermiştir. Test edilen bileşikler arasında 4a'nın, Escherichia coli ve Staphylococcus aureus'a karşı maksimum inhibitör aktiviteleri sırasıyla 6.25 ve 12.5 µg / ml (MIC)'dir. Sentezlenen bileşiklerin moleküler modelleme çalışmaları, bileşiklerin E. coli DNA Gyrase (GyrB) ve DNA Topoizomeraz IV (ParE) alt birimlerinin aktif bölgesindekibağlanma tipini tahmin etmek için gerçekleştirilmiştir. Ayrıca, bileşiklerin ADMET özellikleri hesaplanmıştır.

Anahtar Kelimeler: *Tiyazolopirimidinler, antibakteriyel etki, docking, GyraseB, ParE, sentez.*

Received: 29.06.2018
Revised: 19.08.2018
Accepted: 31.08.2018

[*] Department of Pharmaceutical Chemistry, JSS College of Pharmacy, Udhagamandalam- 643001, Tamil Nadu, India (A Constituent College of JSS Academy of Higher Education & Research, Mysuru).
[**] Department of Pharmaceutical Biotechnology, JSS College of Pharmacy, Udhagamandalam- 643001, Tamil Nadu, India (A Constituent College of JSS Academy of Higher Education & Research, Mysuru).

º Corresponding Author; Unni Jayaram, Department of Pharmaceutical Chemistry, JSS College of Pharmacy, Udhagamandalam- 643001, Tamil Nadu, India (A Constituent College of JSS Academy of Higher Education & Research, Mysuru).
e-mail address: jayaramkvt@gmail.com

INTRODUCTION

The need for the development of newer and potent antibiotics is attributed by the fact that the existing antibacterial agents are facing the problem of bacterial resistance (Azam *et al*., 2015). The existing class of antibiotics are also facing the problem of cross resistance that ensures the need for newer agents that act via novel mechanisms of action or against unique binding sites on existing validated targets (Tari *et al*., 2013). The approach to target multiple sites in the enzyme from multiple essential pathways has gained wide interest in designing novel inhibitors with effective mode of action (Walsh, 2003).The bacterial topoisomerases DNA gyrase (GyrA/GyrB) and topoisomerase IV (ParC/ParE) are promising antibacterial targets that are closely related at the topological levels (Oblak *et al*., 2007). Both topoisomerases form A2B2 holoenzymes that control the topological state of DNA during replication. DNA gyrase is primarily responsible for the initiation of DNA replication and elongation of nascent DNA, while topoisomerase IV is responsible for the decatenation of daughter chromosomal DNA at the end of replication process (Sissi *et al*., 2010). Both synthetic and natural inhibitors are known to bind with multiple discrete binding sites on DNA gyrase (Collin *et al*., 2011). One such classic inhibitor category are the fluoroquinolones that act as topoisomerase poisons by stabilizing a covalent GyrA-DNA complex (Laponogov *et al*., 2010). The aminocoumarin category of inhibitors are known to act via competitive inhibition of GyrB ATPase activity (Heide, 2009). However, this widely utilized antibiotic classes are facing the problem of bacterial resistance and severe adverse effects (Hooper, 2001). The GyrB/ParE ATP-binding subunits still remains largely unexploited which can be utilized as an efficient target for the development of novel antibiotics. Prompted by these findings, we gathered our interest to design some novel synthetic inhibitors that target both enzymes. The known GyrB inhibitors including the coumarins, novobiocin, coumermycin A1, cyclothialidine, cinodine, and clerocidin are proven to show potent action but the problem with poor physicochemical parameters like permeability and water solubility has made them with limited access as antibiotics (Maxwell, 1997). Novobiocin, an aminocoumarin derivative, was shown to inhibit DNA replication by competitively inhibiting the ATPase of both GyrB and ParE subunits (Gellert *et al*., 1976). However, novobiocin showed more affinity towards GyrB subunit. Although toxicity has limited the use of novobiocin, but it showed excellent antibacterial activity for both methicillin-susceptible and -resistant *Staphylococcus aureus* in combination with rifampicin (Walsh *et al*., 1986). This drug combination also prevented the emergence of resistance *in vitro* to each drug in the combination and was found to be useful as mutations to novobiocin resistance in GyrB arised (Walsh *et al*., 1985). Thiazoles and their derivatives have attracted continuing interest over the years because of their varied biological activities including antibacterial action (Ottana *et al*., 2005). In addition, pyrimidine and fused pyrimidine derivatives are one of the most prominent structures found in nucleic acid including uracil, thymine, cytosine, adenine, and guanine, are fundamental building blocks for deoxyribonucleic acid (DNA) and ribonucleic acid (RNA). They also play an essential role in several biological processes, found in nucleoside antibiotics, antibacterials and cardiovascular as well as considerable chemical reactions. The antimicrobial activity of the condensed pyrimidine derivatives have been reported in literatures (Desai *et al*., 2006). Due to the great potential of both of the moiety, the various thiazolopyrimidine derivatives were designed and synthesized to evaluate their antibacterial activity. In the present investigation we aimed to synthesize some novel 3,7-disubstituted-[1,3]thiazolo[4,5-*d*]pyrimidin-2(3*H*)-ones (**2a**, **3a**, **4a** and **4b**) to evaluate their antibacterial activity. We also performed *in silico* molecular docking studies to investigate the binding mode of these compounds with *Escherichia coli* GyrB (PDB ID: 1AJ6) and ParE (PDB ID: 1S14) enzymes.

MATERIALS AND METHODS

The reagents were of commercial grade and used as supplied. Melting points were determined in open glass capillaries and are uncorrected. The reaction progress and purity of the compounds were checked by thin-layer chromatography (TLC) on silica gel F254 plates from Merck. The IR spectra were recorded using a Perkin Elmer FT-IR Spectrum-2 spectrophotometer. The ^{1}H NMR were recorded using Bruker AV-III 400 spectrometer (400 MHZ) with DMSO-d_6 as solvent. Chemical shifts are reported as δ ppm using the solvent as the internal standard. The LC-MS spectra were obtained on Shimadzu 2010A instrument.

Synthesis of 1, 3-thiazolidine-2,4-dione (1):

In a 250 ml three necked flask was placed a solution containing 56.4 g (0.6 mol) of chloroacetic acid in 60 ml of water and 45.6 g (0.6 mol) of thiourea dissolved in 60 ml of water. The mixture was stirred for 15 min and during this time a white precipitate appeared. The contents of the flask was cooled and then 60 ml of concentrated hydrochloric acid was added slowly from a dropping funnel. Gentle heat was applied to effect the solution and the reaction mixture was re-

fluxed with stirring for 8-10 hr at 100-110 ºC. The reaction progress was monitored by TLC. On completion of reaction, the mixture was cooled and separated solid was filtered, washed thoroughly with water and dried. The solid thus obtained was recrystallized from ethanol. Yield 85 %; m.p 123-125 °C (Lit m.p 120-125 °C, Pattan *et al*., 2012); TLC solvent system, acetone: dichloromethane: petroleum ether (2:1:1); R_f value (0.62); IR (KBr) ν cm^{-1}: 3469 (N-H), 2821 (CH_2), 1734, 1648 (C=O), 1339 (C-N), 716 (C-S-C).

Synthesis of 7-(2,4-dihydroxyphenyl)[1,3]thiazolo[4,5-*d*]pyrimidin-2(3*H*)-one (2):

The mixture of 1,3-thiazolidine-2,4-dione (**1**) (0.01 mol; 1.1712 g) and urea (0.01 mol; 0.6005 g) in 15 ml of absolute ethanol was warmed to effect the solution. To the above mixture, 2,4-dihydroxy benzaldehyde (0.01 mol) was added and was refluxed for 8-10 hr. The reaction mixture was cooled and the excess solvent was removed under vacuum and the separated solid was filtered, washed thoroughly with water and recrystallized with ethanol (80 %). Yield 58 %; m.p 130-132 °C; TLC solvent system, acetone: petroleum ether (1:3); R_f value (0.33); IR (KBr) ν cm^{-1}: 3445, 3349 (Ar-OH), 3242 (N-H), 2993 (Ar-H), 1726 (C=O), 1645 (C=N), 895 (C-S-C); ^{1}H-NMR (DMSO-d_6): δ (ppm): 7.97-7.12 (m, 4H, Ar-H), 6.81 (s, 1H, NH), 6.41 (s, 1H, Ar-OH), 6.38 (s, 1H, Ar-OH).

Synthesis of 7-(2,4-dihydroxyphenyl)-3-(2-hydroxyethyl)[1,3]thiazolo[4,5-*d*]pyrimidin-2(3*H*)-one(2a):

To a stirred solution of 7-(2,4-dihydroxyphenyl)[1,3]thiazolo[4,5-*d*]pyrimidin-2(3*H*)-one (**2**) (0.0038 mol; 1 g) in dry acetone (5 ml) was added anhydrous K_2CO_3 (0.0038 mol; 0.53 g) and this mixture was stirred at room temperature for 1 hr. Then 2-bromoethanol (0.0038 mol; 0.27 ml) was added and the reaction mixture was further stirred at 40 °C for 13 hr. After completion of reaction, excess of solvent was removed in vacuum and the separated solid was filtered and recrystallized with ethanol-water mixture (1:1). Yield 41 %; m.p 210-212 °C; TLC solvent system, acetone: petroleum ether (2:3); R_f value (0.45); IR (KBr) ν cm^{-1}: 3263 (Ar-OH), 1693 (C=O), 1610 (C=N), 1437 (C-N); ^{1}H-NMR (DMSO-d_6): δ (ppm): 7.66-6.81 (m, 4H, Ar-H), 6.17 (s, 1H, Ar-OH), 6.15 (s, 1H, Ar-OH), 3.61 (t, 2H, OCH_2), 3.48 (t, 2H, -NCH_2), 1.13 (s, 1H, aliphatic OH); LC-MS (ESI): m/z calculated for $C_{13}H_{11}N_3O_4S$: 305. Found: m/z 308. ($M^{+\cdot}$+3H^+), 287, 275, 203, 171, 141, 121 (base peak), 71.

Synthesis of [7-(2,4-dihydroxyphenyl)-2-oxo[1,3]thiazolo[4,5-*d*]pyrimidin-3(2*H*)-yl]acetyl chloride (3):

To an ice cold solution of 7-(2,4-dihydroxyphenyl)[1,3]thiazolo[4,5-*d*]pyrimidin-2(3*H*)-one (**2**) (0.0038 mol; 1 g) in dry toluene (10 ml) was added chloroacetyl chloride (0.0076 mol; 0.62 ml) dropwise with constant stirring. After addition of chloroacetyl chloride, stirring was further continued until completion of reaction (5 hr). The reaction mixture was poured over crushed ice and the separated solid was filtered, washed several time with water and recrystallized with ethanol. Yield 69 %; m.p 280-285 °C; TLC solvent system, acetone: petroleum ether (2:3); R_f value (0.27); IR (KBr) ν cm^{-1}: 3500 (Ar-OH), 3127, 3030 (Ar-H), 1681 (C=O), 911 (C-S-C), 694 (C-Cl); ^{1}H-NMR (DMSO-d_6): δ (ppm): 8.06-7.32 (m, 4H, Ar-H), 6.57 (s, 1H, Ar-OH), 6.45 (s, 1H, Ar-OH), 4.17 (s, 2H, CH_2).

Synthesis of 2-[7-(2,4-dihydroxyphenyl)-2-oxo[1,3]thiazolo[4,5-*d*]pyrimidin-3(2*H*)-yl]-*N*,*N*-diethylacetamide (3a):

To a stirred mixture of [7-(2,4-dihydroxyphenyl)-2-oxo[1,3]thiazolo[4,5-*d*]pyrimidin-3(2*H*)-yl]acetyl chloride (**3**) (0.00296 mol; 1 g) and anhydrous K_2CO_3 (0.003 mol; 0.4 g) in dry acetone (15 ml) was added diethyl amine (0.00296 mol; 0.2165 g) dropwise. Stirring was further continued at room temperature for 5 hr. On completion of reaction, excess of solvent was removed in vacuum and the separated solid was recrystallized with ethanol. Yield 48 %; m.p 150-152 °C; TLC solvent system, acetone: ethyl acetate (2:3); R_f value (0.42); IR (KBr) ν cm^{-1}: 3222 (Ar-OH), 1687, 1588 (C=O), 1439 (C-N), 901 (C-S-C); ^{1}H-NMR (DMSO-d_6): δ (ppm): 7.52-7.27 (m, 4H, Ar-H), 6.82 (s, 1H, Ar-OH), 6.25 (s, 1H, Ar-OH), 3.35 (s, 2H, O=C-CH_2N-), 2.73-2.48 (m, 4H, -N-CH_2), 1.98-1.06 (m, 6H, -CH_3); LC-MS (ESI): m/z calculated for $C_{17}H_{18}N_4O_4S$: 374. Found: m/z 372. ($M^{+\cdot}$-2H^+), 357, 342, 279, 228, 202, 115 (base peak), 74.

Synthesis of 3-(3-hydroxypropyl)-1,3-thiazolidine-2,4-dione (4):

To a stirred solution of 1,3-thiazolidine-2,4-dione (**1**) (0.05 mol; 5.86 g) in dry acetone (40 ml) was added anhydrous K_2CO_3 (0.1 mol; 13.8 g) and the mixture was stirred at room temperature for 1 hr. Then 3-bromopropanol (0.1 mol; 8.87 ml) was added dropwise and the reaction mixture was further stirred at 40 °C for 15 hr. On completion of reaction, excess of solvent was removed in vacuum and the separated solid was recrystallized with ethanol (U.S. Patent Application No. 2008/0076760A1, 2008). Yield 71 %; m.p 240-245 ºC; TLC solvent system, acetone: dichloromethane: petroleum ether (2:1:3); R_f value (0.45); IR (KBr) ν cm^{-1}: 3498 (O-H), 3010 (Ar-H), 2825 (CH_2), 1658 (C=O), 922 (C-S-C).

Synthesis of 7-(2,4-dihydroxyphenyl)-3-(3-hydroxypropyl)[1,3]thiazolo[4,5-*d*]pyrimidin-2(3*H*)-one (4a):

To a stirred mixture of 3-(3-hydroxypropyl)-1,3-thiazolidine-2,4-dione (**4**) (0.0057 mol; 1 g) and urea (0.0057 mol; 0.34 g) in absolute ethanol (8 ml) was added 2,4-dihydroxybenzaldehyde (0.0057 mol; 0.7873 g). The reaction mixture was refluxed for 8-10 hr. Then excess solvent was removed under vacuum and the separated solid was filtered and washed several time with water and recrystallized with acetone. Yield 62 %; m.p 203-205 °C; TLC solvent system, acetone: petroleum ether (1:4); R_f value (0.45); IR (KBr) ν cm^{-1}: 3269 (Ar-OH), 3010 (Ar-H), 2830 (CH_2), 1716 (C=O), 1614 (C=N), 1438 (C-N), 973 (C-S-C); ^{1}H-NMR (DMSO-d_6): δ (ppm): 9.83-7.95 (m, 4H, Ar-H), 6.45 (s, 1H, Ar-OH), 6.42 (s, 1H, Ar-OH), 4.16 (t, OCH_2), 3.34 (t, NCH_2), 2.73 (q, 2H), 2.50 (s, 1H, aliphatic OH); LC-MS (ESI): m/z calculated for $C_{14}H_{13}N_3O_4S$: 319. Found: m/z 316. ($M^{+\cdot}$-3H^+), 302, 288 (base peak), 209, 192, 84.

Synthesis of 3-(3-hydroxypropyl)-7-(4-nitrophenyl)[1,3]thiazolo[4,5-*d*]pyrimidin-2(3*H*)-one (4b):

To a stirred mixture of 3-(3-hydroxypropyl)-1,3-thiazolidine-2,4-dione (**4**) (0.0057 mol; 1 g) and urea (0.0057 mol; 0.34 g) in absolute ethanol (8 ml) was added 4-nitrobenzaldehyde (0.0057 mol; 1.299 g). The reaction mixture was refluxed for 8-10 hr. Then excess solvent was removed under vacuum and the separated solid was filtered and washed several time with water and recrystallized with ethyl alcohol. Yield 59 %; m.p 179-181 °C; TLC solvent system, acetone: petroleum ether (2:3); R_f value (0.44); IR (KBr) ν cm^{-1}: 3400 (Ar-OH), 3303 (Ar-H), 1646 (C=O), 1512 (C=N), 1054 (C-N), 872 (C-S-C); ^{1}H-NMR (DMSO-d_6): δ (ppm): 8.43-7.24 (m, 5H, Ar-H), 3.34 (t, OCH_2), 3.08 (t, NCH_2), 2.50 (q, 2H, CH_2), 1.97 (s, 1H, OH); LC-MS (ESI): m/z calculated for $C_{14}H_{12}N_4O_4S$: 332. Found: m/z 380. ($M^{+\cdot}$-2H^++H_2O+CH_3CN), 288, 248 (base peak), 209, 192, 86.

MOLECULAR DOCKING STUDIES

Ligand preparation

The chemical structures of synthesized molecules (**2a**, **3a**, **4a** and **4b**) along with the standard drug novobiocin were prepared using ACD/chemsketch freeware. Prior to the computational studies, the 3-dimensional (3D) structures of the ligands were energy optimized using Ligprep module in Schrödinger suite (2017-2). The 3D conversion and energy minimization was performed using optimized potential for liquid simulations (OPLS3) force field (Greenwood *et al*., 2010). The Ligprep optimizes the input ligand structures to global minima by adding hydrogens, removing counter ions and by generating distinct ionization states and stereoisomers (Shivakumar *et al*., 2010). The energy minimization was performed with relative window of 10 kcal mol^{-1} and RMSD of 1 Å using the OPLS3 force field (Greenwood *et al*., 2010).

Protein preparation and molecular docking

The X-ray crystallography derived structures of the target enzymes *E. coli* GyrB (PDB ID: 1AJ6, resolution: 2.3 Å) and ParE (PDB ID: 1S14, resolution: 2 Å) were retrieved from the protein data bank. These proteins were prepared using Protein Preparation Wizard tool (Sastry *et al*., 2013) in Schrödinger suite 2017-2. The structures were pre-processed to assign the bond orders and zero order bonds to metals. The missing side chains were added and break up in protein structures were repaired using prime (v4.8) (Jacobson *et al*., 2004) module. Energy minimization of protein structures were performed using OPLS3 force field. The crystallographic water molecules with less than three hydrogen bonds were deleted. Hydrogen bonds were assigned keeping the crystal symmetry and minimization of hydrogens of altered species as default. Finally, the restrained minimization was performed until the convergence of heavy atoms reached to 0.30 Å RMSD. The active sites were defined with a 10 Å radius around the co-crystal ligand present in the crystal structure of the respective enzymes and a grid box was generated at the centroid of the active site of the respective enzymes. To test the docking parameters, low energy conformations of all compounds were docked into the catalytic pocket of the selected enzymes using grid based ligand docking with energetics (Glide v7.5) (Friesner *et al*., 2006) in 'extra precision'(XP) mode without applying any constraints.

Prediction of ADME descriptors and toxicity

All the designed ligands were screened on the basis of absorption, distribution, metabolism, excretion (ADME) and toxicity filter using QikProp module incorporated in Schrödinger software (2017-2). Output of QikProp showed a number of principal descriptors and ADME properties. Various physicochemical properties were calculated, represented by different descriptors such as molecular weight (mol_MW), number of rotatable bonds (#rotor), lipophilicity parameter (QPlogPo/w), number of hydrogen bond acceptors (accptHB), number of hydrogen bond donors (donorHB), total polar surface area (PSA), solubility (log S), solvent

accessible surface area (SASA), binding to human serum albumin (QPlogKhsa), percentage human oral absorption (Percent Human-Oral Absorption).

ANTIBACTERIAL SCREENING

Determination of zone of inhibition

The antibacterial activities of the synthesized compounds against five pathogenic bacteria (three Gram-positive and two Gram-negative) were investigated by the agar disk diffusion method (Barry, 1999). The tested strains include Gram-positive (*Bacillus subtilis* NCIM 2063, *S. aureus* NCIM 5021 and *S. aureus* NCIM 5022) and Gram-negative (*Pseudomonas aeruginosa* NCIM 2200 and *E. coli* NCIM 2065) bacteria. Each synthesized compounds along with the standard drugs methicillin and amoxicillin, were dissolved in dimethyl sulfoxide, and stored at 4 °C. All the compounds were screened for their antibacterial activities against the selected strains. Mueller Hinton sterile agar plates were seeded with indicator bacterial strains (10^8 CFU) and allowed to stay at 37 °C for 3 hours. Control experiments were carried out under similar condition by using methicillin and amoxicillin as the standard drugs. The zones of growth inhibition were measured after 18 to 24 hr of incubation at 37 °C for bacteria. The sensitivities of the bacteria to the compounds were determined by measuring the sizes of inhibitory zones on the agar surface.

Determination of minimum inhibitory concentration (MIC)

The MIC values were determined by broth dilution method and as per the guidelines of Clinical and Laboratory Standards Institute, with some modifications (Barry, 1999). The sets of seven dilutions (1.56, 3.125, 6.25, 12.5, 25, 50 and 100 µg/ml) of compounds and standards were prepared in millipore double distilled water using nutrient agar tubes. A control test was also performed containing inoculated broth supplemented with only dimethyl sulphoxide at the same dilutions used in our experiments and found inactive in the culture medium. The cultures were obtained from Mueller-Hinton broth for all the bacterial strains after 24 hr of incubation at 37 ± 1 °C. Testing was carried out in Mueller-Hinton broth at pH 7.4 and the two fold serial dilution technique was applied. The final inoculum size was 10^5 CFU/ml for the antibacterial assay. A set of tubes containing only inoculated broth was used as controls. For the antibacterial assay after incubation for 24 hr at 37 ± 1 °C, the tube with no visible growth of microorganism was recorded to represent the MIC and expressed in µg/ml. Every experiment was replicated thrice.

RESULTS AND DISCUSSION

CHEMISTRY

Reaction route for the synthesis of title compounds **2a**, **3a**, **4a** and **4b** is outlined in Figure 1. 1,3-thiazolidine-2,4-dione (**1**) was synthesized by the reaction of chloroacetic acid and thiourea in water in the presence of hydrochloric acid by literature method (Pattan *et al*., 2012). The key intermediate 7-(2,4-dihydroxyphenyl)[1,3]thiazolo[4,5-*d*]pyrimidin-2(3*H*)-one (**2**) was prepared by the reaction of urea, 1,3-thiazolidine-2,4-dione (**1**) and 2,4-dihydroxybenzaldehyde in reflux with absolute ethanol. The reaction of compound **2** with 2-bromoethanol in presence of anhydrous K_2CO_3 in acetone gave the title compound 7-(2,4-dihydroxyphenyl)-3-(2-hydroxyethyl)[1,3]thiazolo[4,5-*d*]pyrimidin-2(3*H*)-one (**2a**). The reaction of compound **2** with chloroacetyl chloride in dry toluene furnished the intermediate [7-(2,4-dihydroxyphenyl)-2-oxo[1,3]thiazolo[4,5-*d*]pyrimidin-3(2*H*)-yl]acetyl chloride (**3**) which on further reaction with diethylamine in acetone yielded the title compound 2-[7-(2,4-dihydroxyphenyl)-2-oxo[1,3]thiazolo[4,5-*d*]pyrimidin-3(2*H*)-yl]-*N*,*N*-diethylacetamide (**3a**). The key intermediate, 3-(3-hydroxypropyl)-1,3-thiazolidine-2,4-dione (**4**) was synthesized by reaction of **1** with 3-bromopropanol in the presence of anhydrous K_2CO_3 in acetone. The reaction of compound **4** with urea and 2,4-dihydroxybenzaldehyde in absolute ethanol yielded compound 7-(2,4-dihydroxyphenyl)-3-(3-hydroxypropyl)[1,3]thiazolo[4,5-*d*]pyrimidin-2(3*H*)-one (**4a**) whereas reaction of compound **4** with urea and 4-nitrobenzaldehyde in absolute ethanol gave compound 3-(3-hydroxypropyl)-7-(4-nitrophenyl)[1,3]thiazolo[4,5-*d*]pyrimidin-2(3*H*)-one (**4b**). The physical characterization data of the synthesized compounds has been included in Table 1. The structures of final compounds were characterized by means of FT-IR, ^{1}H-NMR and LC-MS data. In the FT-IR spectrum of compound **1**, appearance of -NH, -CH_2 alicyclic, >C=O, C-N and C-S-C stretching bands were observed at 3469, 2821, 1734, 1339 and 716 cm^{-1}, respectively. In the FT-IR spectrum of compound **2**, appearance of -OH aromatic, -NH amide, Ar-H, >C=O, C=N and C-S-C stretching bands were observed at 3445, 3242, 2993, 1726, 1645 and 895 cm^{-1} respectively. In case of final compound **2a**, the IR peaks were observed at 3263 (Ar-OH), 1693 (C=O), 1610 (C=N), 1437 (C-N) cm^{-1} in FT-IR spectrum. ^{1}H-NMR spectrum of the compound **2a** showed multiplet at δ 7.66-6.81 ppm corresponding to four aromatic and one pyrimidinyl proton. The singlet signals observed at δ 6.17 (s, 1H,

Ar-OH) and 6.15 (s, 1H, Ar-OH) ppm were assigned, respectively for two protons from OH groups and two triplet signals observed at 3.48 and 3.61 were assigned to NCH_2 and OCH_2 protons. The aliphatic side chain -OH proton showed a singlet at δ 1.13 ppm. The FT-IR spectrum of compound **3** showed the appearance of -OH, Ar-H, >C=O, C-S-C and C-Cl stretching bands at 3500, 3127, 1681, 911 and 694 respectively. In the FT-IR spectrum of compound **3a**, characteristic IR stretching bands were observed at 3222 (Ar-OH), 1687 and 1588 (C=O), 1439 (C-N), 901 (C-S-C) cm^{-1}. Formation of compound **3a** was further supported by the disappearance of C-Cl stretching band at 694 cm^{-1}. In the FT-IR spectrum of compound **4** appearance of stretching bands at 3498 (OH), 3010 (Ar-H), 2825 (CH_2 aliphatic), 1658 (C=O) and 922 (C-S-C) cm^{-1} supported the formation of 1,3-thiazolidine-2,4-dione nucleus with alkyl hydroxyl side chain. Formation of [1,3]thiazolo[4,5-*d*]pyrimidin-2(3*H*)-one nucleus in compound **4a** was supported by the appearance of bands at 3269 (Ar-OH), 3010 (Ar-H), 2830 (CH_2 aliphatic), 1716 (C=O), 1614 (C=N), 1438 (C-N) and 973 (C-S-C) cm^{-1}. The ^{1}H-NMR spectrum of same compound showed a multiplet at δ 9.83-7.95 ppm integrating for four protons is assigned to the aromatic and pyrimidinyl protons. A singlet signal observed at δ 6.45 ppm and δ 6.42 ppm were assigned to the protons from aromatic hydroxyl groups. Two triplet signals observed at 4.16 and 3.34 ppm were due to OCH_2 and NCH_2 fragment whereas a quintet signal appeared at 2.73 ppm was assigned to the $-CH_2-$ fragment. In the FT-IR spectrum of compound **4b**, IR stretching bands were observed at 3400 (OH), 3303 (Ar-H), 1646 (C=O), 1512 (C=N), 1054 (C-N), 872 (C-S-C) cm^{-1}. In the ^{1}H-NMR spectrum of same compound a multiplet observed in the range at δ 8.43-7.24 ppm was ascribed to the five aromatic protons. The singlet signal obtained at δ 1.97 ppm was assigned to one aliphatic hydroxyl proton. Two triplet and a quintet signal appeared at 3.34, 3.08 and 2.50 ppm integrating for two protons each were assigned, respectively to $-OCH_2$, NCH_2, $-CH_2$ fragments.

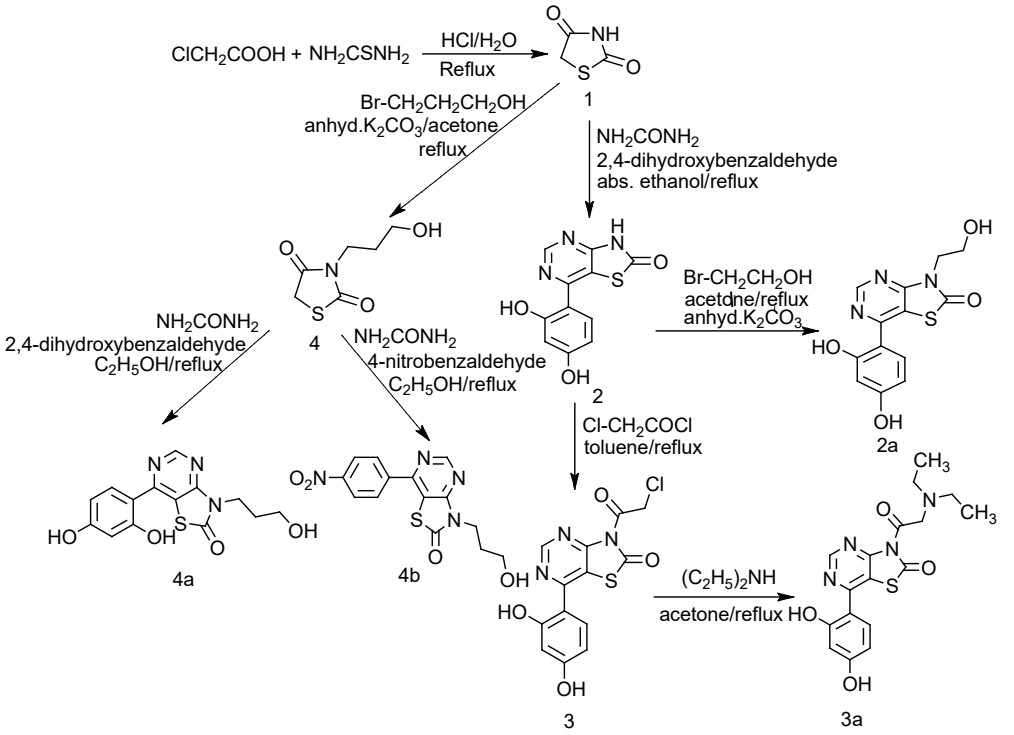

Figure 1. The scheme for the synthesis of titled compounds (**2a**, **3a**, **4a** and **4b**).

Table 1. The physical characterization data of the derivatives and synthesized compounds.

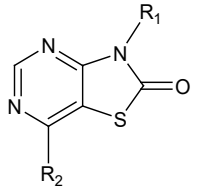

Compound	R_1	R_2	Molecular formula	Mol. weight	M.P. (°C)	Yield (%)
2	H	2,4-di-OH.C_6H_3	$C_{11}H_7N_3O_3S$	261.26	130-132	58
2a	CH_2CH_2OH	2,4-di-OH.C_6H_3	$C_{13}H_{11}N_3O_4S$	305.30	210-212	41
3	$COCH_2Cl$	2,4-di-OH.C_6H_3	$C_{13}H_8ClN_3O_4S$	337.74	280-285	69
3a	$COCH_2N(C_2H_5)_2$	2,4-di-OH.C_6H_3	$C_{17}H_{18}N_4O_4S$	374.41	150-152	48
4a	$CH_2CH_2CH_2OH$	2,4-di-OH.C_6H_3	$C_{14}H_{13}N_3O_4S$	319.34	203-205	62
4b	$CH_2CH_2CH_2OH$	4-NO_2.C_6H_4	$C_{14}H_{12}N_4O_4S$	332.33	179-181	59

MOLECULAR DOCKING

The prepared protein was validated using the Ramachandran plot (Fig. 2). In case of GyrB (PDB ID: 1AJ6), 95.89 % of total amino acids were found to be in acceptable region. On the other hand, 98.45 % of total amino acids were found to be in acceptable region for ParE (PDB ID: 1S14). To study the binding modes of synthesized molecules **2a**, **3a**, **4a** and **4b**, docking results are compared and summarized in Table 2 and Table 3. The molecular docking data clearly suggested that the synthesized molecules bind well with GyrB and ParE. In case of GyrB synthesized compounds exhibited hydrogen bonding interactions with key binding residues Asn46, Glu50, Asp73, Arg76, Gly77 and Thr165, whereas in case of ParE, interactions were with Asn1042, Asp1069 and Gly1073. In case of compound **2a**, 2-OH group of aryl ring present at seventh position of the thiazolopyrimidine ring formed hydrogen bond (2.09 Å) with carbonyl oxygen of Asn46, while the aliphatic side chain -OH group present at third position of the thiazolopyrimidine ring formed hydrogen bond (2.19 Å) with >C=O of Glu50. In compound **3a**, a stable π-cationic interaction was observed between position seven aryl ring and -NH of Arg76. The position two >C=O group of thiazolopyrimidine scaffold exhibited hydrogen bond (2.23 Å) with -NH of Gly77. Similar to **3a**, position seven aryl ring of compound **4a** showed π-cationic interaction with -NH of Arg76. Moreover, a hydrogen bond (2.07 Å) was observed between position two >C=O group of thiazolopyrimidine scaffold and -NH of Gly77. In addition to this, the position two >C=O group of thiazolopyrimidine scaffold also exhibited hydrogen bond (1.87 Å) with -OH of Thr165. The aliphatic side chain -OH group present at third position of the thiazolopyrimidine ring also exhibited hydrogen bond (1.81 Å) with >C=O of Asp73. In compound **4b**, the position two >C=O group and third position aliphatic side chain -OH group exhibited hydrogen bonding interactions with the binding site residues Asp73 (1.83 Å), Gly77 (2.29 Å) and Thr165 (2.10 Å). However, the 4-NO_2 of phenyl ring present at position seven of the thiazolopyrimidine scaffold exhibited two hydrogen bonding interaction with Arg76. The extra-precision docking poses within the catalytic pocket of 1AJ6 is provided in Figure 3.

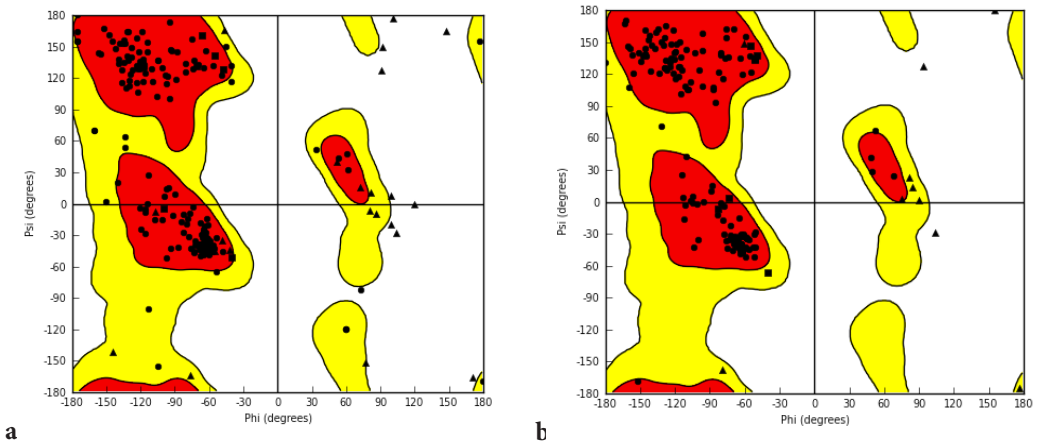

Figure 2. The Ramachandran plots of a) DNA Gyrase GyrB (PDB ID: 1AJ6) and b) DNA Topoisomerase IV ParE (PDB ID: 1S14).

Table 2. Docking of 3,7-disubstituted-[1,3]thiazolo[4,5-*d*]pyrimidin-2(3*H*)-ones in the active site of bacterial DNA Gyrase Gyr B (PDB ID: 1AJ6).

Compound	[a]Glide gscore	[b]Glide evdw	[c]Glide ecoul	[d]Glide energy	[e]Glide emodel	Interacting amino acids
2a	-4.648	-29.51	-5.51	-35.02	-49.798	Asn46, Glu50
3a	-6.602	-37.46	-7.83	-45.29	-58.717	Asp73, Arg76, Gly77
4a	-4.309	-32.79	-7.8	-40.62	-55.060	Arg76, Asp73, Gly77, Thr165
4b	-4.298	-35.83	-9.00	-44.84	-62.154	Asp73, Arg76, Gly77, Thr165
novobiocin	-6.046	-35.20	-12.4	-47.61	-63.006	Glu50, Asp73, Arg76

Notes: [a]Glide score; [b]van der Waals energy; [c]Coulomb energy; [d]Glide binding energy; [e]Glide model energy.

Table 3. Docking of 3,7-disubstituted-[1,3]thiazolo[4,5-*d*]pyrimidin-2(3*H*)-ones in the active site of bacterial Topoisomerase IV ParE (PDB ID: 1S14).

Compound	[a]Glide gscore	[b]Glide evdw	[c]Glide ecoul	[d]Glide energy	[e]Glide emodel	Interacting amino acids
2a	-4.802	-26.37	-5.50	-31.87	-36.196	Asp1069
3a	-5.470	-42.29	-0.08	-42.38	-44.417	Asp1069
4a	-5.670	-31.68	-4.95	-36.637	-42.781	Gly1073
4b	-5.514	-37.52	-5.06	-42.582	-50.095	Asn1042
Novobiocin	-4.954	-28.26	-9.02	-37.276	-54.457	Asn1042, Asp1077, Ile1078, Arg1132,

[a]Glide score; [b]van der Waals energy; [c]Coulomb energy; [d]Glide binding energy; [e]Glide model energy (Emodel has a more significant weighting of the force field componentsand is well-suited for comparing conformers to pick the "best" pose of a ligand).

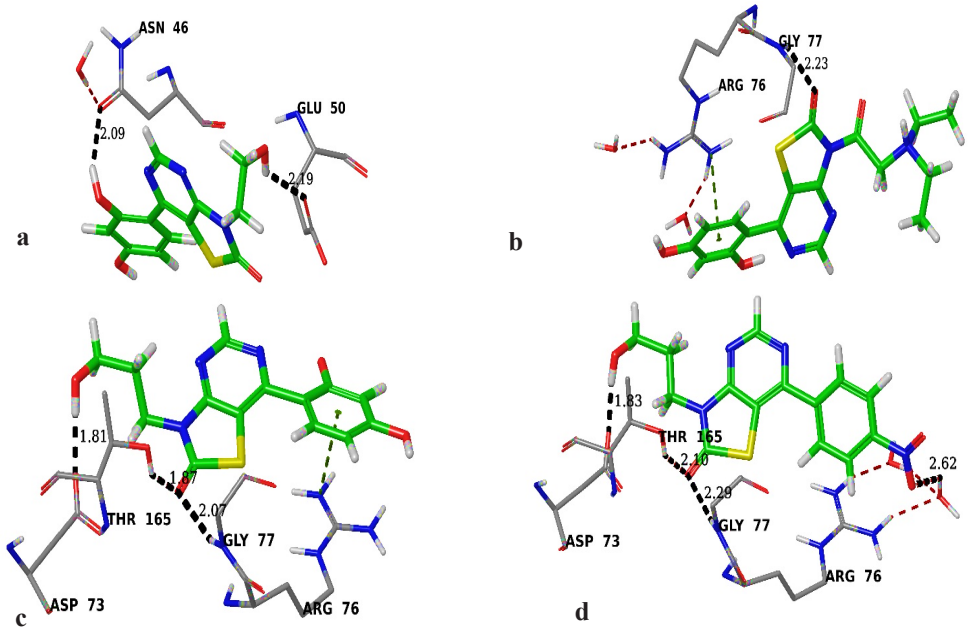

Figure 3. The binding pose and interaction of the synthesized test compounds, a) **2a**, b) **3a**, c) **4a** and d) **4b** within the catalytic pocket of DNA Gyrase GyrB (PDB ID: 1AJ6).

The extra-precision docking pose of compound **2a** in the catalytic pocket of ParE enzyme (PBD-ID: 1S14) showed hydrogen bonding (1.79 Å) interaction between aliphatic side chain -OH and carboxylate oxygen of Asp1069. The same -OH group also formed water molecule (3) mediated hydrogen bond with the carbonyl oxygen of (2.01 Å) of Asp1069. This water molecule is also involved in hydrogen bond bridge interaction with Asp1069. In compound **3a**, 2-OH group of phenyl ring present at seventh position of the thiazolopyrimidine ring formed two hydrogen bonds (2.24 Å) with carboxylate oxygen atoms of Asp1069. The position six nitrogen atom of thiazolopyrimidine scaffold also exhibited water bridged interactions with Gly1073, Thr1163 and Asp1069 residues. The aliphatic side chain -OH of compound **4a** accepted a hydrogen bond (2.21 Å) from the carbonyl oxygen of Gly1073. In compound **4b**, a hydrogen bonding interaction was observed between -OH of -$CH_2CH_2CH_2OH$ fragment and -NH of Asn1042 (2.05 Å). The binding pose and interaction of the test molecules within the catalytic pocket of 1S14 is provided in Figure 4.

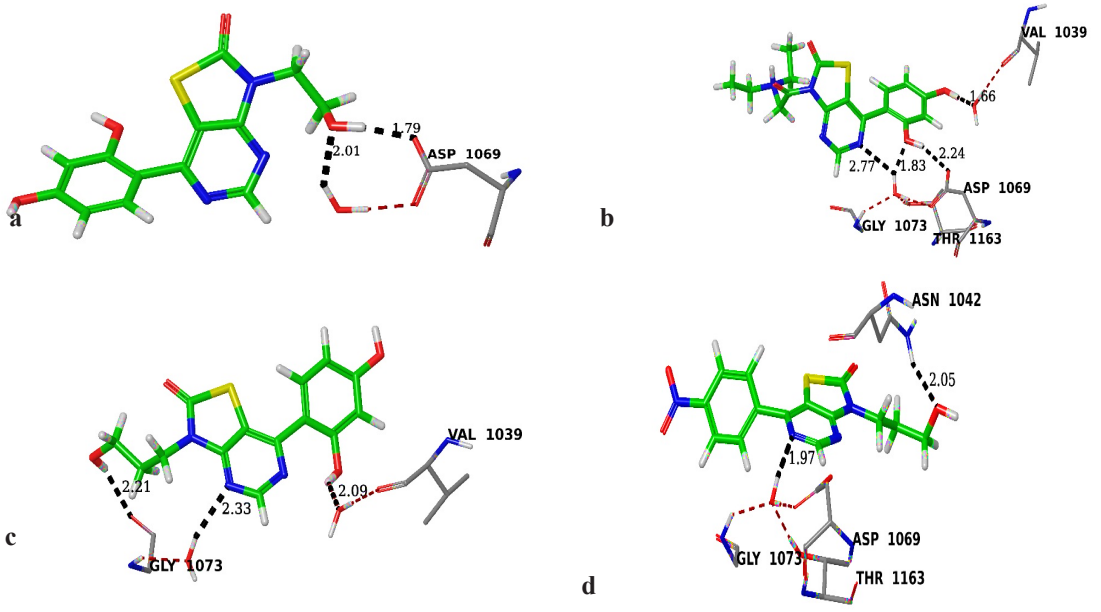

Figure 4. The binding pose and interaction of the synthesized test compounds, a) **2a**, b) **3a**, c) **4a** and d) **4b** within the catalytic pocket of DNA Topoisomerase IV ParE (PDB ID: 1S14).

The Gscore values (a scoring function that approximates the ligand binding free energy), of the synthesized compounds were in the range -4.298 to -6.602 kcal mol^{-1} in case of 1AJ6, while values was in the range -4.802 to -5.670 kcal mol^{-1} in case of 1S14. In 1AJ6, the compound **3a** showed higher Gscore value of -6.602 kcal mol^{-1} compared to the standard drug novobiocin (-6.046 kcal mol^{-1}). In case of 1S14, all compounds except **2a**, exhibited high Gscore values compared to the novobiocin (-4.954 kcal mol^{-1}). In case of 1AJ6, compounds showed Glide energy in the range -35.02 to -45.29 kcal mol^{-1}. This was slightly lower in comparison to that of novobiocin (-47.61 kcal mol^{-1}). For the ParE protein (1S14), novobiocin showed comparatively lower Glide energy of -37.276 kcal mol^{-1}, compared to the synthesized compounds (-31.87 to -42.58 kcal mol^{-1}). The high negative Glide energy values exhibited by the synthesized compounds ensure a perfect fit at the catalytic pocket of concerned enzymes. Coulomb and van der Waals energies, used for the post-docking minimization, is also computed (Table 2 and 3).

Further, we computed ADMET properties to assess the safety of titled compounds **2a**, **3a**, **4a** and **4b** (Table 4). The predicted central nervous system (CNS) activity of all screened compounds were observed to be -2 which is in the acceptable range of -2 to +2. The value of total solvent accessible surface area (SASA) ranged from 504.94 to 644.31 $Å^2$ which is well within the acceptable range of 300.0-1000.0 $Å^2$. In general, SASA provides a useful tool for predicting overall extent of hydrophobic region on a molecule or in the binding site of a protein. In most cases, increase in the SASA value of a compound, causes considerable increase in its activity. Hydrogen bonding is most likely an essential requirement for many drug-receptor interactions. The number of hydrogen bonds donated (donorHB) by the solute to water molecules were found to be in 1 to 3 range, and the hydrogen bonds accepted (accptHB) by the solute were found in the range 7 to 9. The predicted octanol/water partition coefficient (QPlogPo/w) ranged from 0.30 to 1.19 which is well within the recommended range of -2.0 to 6.5. The predicted human oral absorption showed excellent values ranging from 62.60 to 70.70 %. Finally, QPlogHERG values for compounds **2a**, **3a** and **4a** was observed to be -4.47, -3.87 and -4.89, respectively, indicating the lower affinity of these molecules towards HERG K^+ channels and hence cardiac effects. However, there is little concern about compound **4b**, showing QPlogHERG value of -5.24.

Table 4. The Qikprop data of the synthesized molecules for predicting the ADME properties.

Comp	Mol.wt.	CNS activity	Donor H-bond	Acceptor H-bond	QPlog HERG	Human oral absorption (%)	QPlogPo/w	SASA ($Å^2$)
2a	305.30	-2	3	8	-4.47	62.60	0.30	504.94
3a	374.41	-2	2	9	-3.87	70.70	0.93	644.31
4a	319.34	-2	3	8	-4.89	67.11	0.61	557.86
4b	332.33	-2	1	7	-5.24	65.85	1.19	576.84

CNS: The predicted central nervous system activity on a -2 (inactive) to +2 (active) scale; Donor H-bond: The number of hydrogen bonds that would be donated by the compound; Acceptor H-bond: The number of hydrogen bonds that would be accepted by the compound; QPlogHERG: Predicted IC_{50} value for the HERG K^+ channels blockage (concern below -5); Predicted human oral absorption on 0 to 100 % scale (>80 % is high, <25 % is poor); QPlogPo/w: Predicted octanol/water partition coefficient; SASA: Total solvent accessible surface area in square angstroms using a probe with a 1.4 Å radius.

ANTIBACTERIAL ACTIVITY

Determination of zone of inhibition

To evaluate the potency of the synthesized molecules as antibacterial agents, the zone of inhibition exhibited by tested compounds at 100 µg/ml were determined and compared with standard drugs methicillin and amoxicillin (100 µg/ml). The test compounds showed high activity against Gram-positive bacteria (*B. subtilis* NCIM 2063, *S. aureus* NCIM 5021 and *S. aureus* NCIM 5022), when compared to the Gram-negative bacteria (*P. aeruginosa* NCIM 2200 and *E. coli* NCIM 2065). The standard drug methicillin showed high inhibitory activity against *S. aureus* NCIM 5022 (zone of inhibition: 24 mm) and *P. aeruginosa* NCIM 2200 (zone of inhibition: 22 mm). On the other hand, amoxicillin showed potent activity against all selected strains (zone of inhibition: 20-32 mm). The synthesized molecules showed significant activity (zone of inhibition: 13-15 mm) compared to the standard drug methicillin (zone of inhibition: 15 mm) against *S. aureus* NCIM 5021. In case of *B. sub-*

tilis NCIM 2063, the molecules (zone of inhibition: 12-14 mm) showed moderate activity in comparison to the standard drug amoxicillin (zone of inhibition: 32 mm). Methicillin did not exhibit significant activity against *E. coli* NCIM 2065 (zone of inhibition: 13 mm). However, the compounds **3a** and **4a** showed high inhibitory activity (zone of inhibition: 12 mm) against *E.coli* NCIM 2065, compared to the methicillin. Maximum antibacterial activity was exhibited by synthesized molecules towards *S. aureus* NCIM 5021 and *S. aureus* NCIM 5022 (zone of inhibition: 12-15 mm) when compared to the standard drugs methicillin (*S. aureu*s NCIM 5021, zone of inhibition: 15 mm; *S. aureus* NCIM 5022, zone of inhibition: 24 mm) and amoxicillin (*S. aureus* NCIM 5021, zone of inhibition: 22 mm; *S. aureu*s NCIM 5022, zone of inhibition: 30 mm). Although none of the test compounds showed activity comparable to that of known antibacterial standard drugs, the test compound **3a** showed promising inhibitory activity against *S. aureus* NCIM 5021, *S. aureus* NCIM 5022, *B. subtilis* NCIM 2063 and *E. coli* NCIM 2065. The test compounds **2a** and **4a** differ only in terms of one extra -CH_2 group in the side chain of their chemical structure. Compound **2a** having one -CH_2 less than that of **4a** in third position of the thiazolopyrimidine ring, was able to exhibit significant antibacterial activity towards the Gram-positive strains. However, the extra -CH_2 in **4a**, diminished its antibacterial potency. Interestingly, compound **4a** exhibited moderate activity (zone of inhibition: 12 mm) towards the Gram-negative strain *E. coli* NCIM 2065. When 2-hydroxy ethyl side chain in third position of the thiazolopyrimidine ring in **2a** is replaced with *N,N*-diethyl acetamide side chain (**3a**), the antibacterial activity slightly increased against Gram- positive strains *S. aureus* NCIM 5021 and *S. aureus* NCIM 5022 (zone of inhibition: 15 mm in both cases). The compound **3a** also showed enhanced activity against Gram-negative bacteria *E. coli* NCIM 2065 (zone of inhibition: 12 mm) which was absent in case of **2a**. The zone of inhibition studies suggested that the substitution of 2,4-dihydroxy phenyl ring at position seven and, *N,N*-diethyl acetamide side chain at position three of thiazolopyrimidine ring as in case of compound **3a**, is optimal for bacterial activity against Gram-positive *S. aureus* NCIM 5021, *S. aureus* NCIM 5022 and *B. subtilis* NCIM 2063 and Gram-negative *E. coli* NCIM 2065. It is also evident from results that molecules having electron donating groups like -OH group attached to the phenyl ring of the substituted thiazolopyrimidine scaffold may enhance the inhibitory activity against the selected test strains. The zone diameters in mm are listed in Table 5.

Table 5. The antibacterial activities of synthesized molecules and standard drugs against selected strains of microorganisms.

Compound	Zone of inhibition (mm)[a]				
	S.a 5021[b]	*S.a* 5022[c]	*B.s* 2063[d]	*E.c* 2065[e]	*P.a* 2200[f]
2a	13	13	14	-	-
3a	15	15	12	12	-
4a	-	-	-	12	-
4b	13	12	-	-	-
methicillin	15	24	15	13	22
amoxicillin	22	30	32	20	22

[a]Values are mean ± SD of three parallel measurements.
[b]*S.a.*: *Staphylococcus aureus* (NCIM 5021); [c]*S.a.*: *Staphylococcus aureus* (NCIM 5022); [d]*B.s.*: *Bacillus subtilis* (NCIM2063); [e]*E.c.*: *Escherichia coli* (NCIM 2065); [f]*P.a.*: *Pseudomonas aeruginosa* (NCIM 2200). The test compounds, methicillin and amoxicillin were used at 100 µg/ml concentration.
-: not determined.

Determination of minimum inhibitory concentration (MIC)

The MIC values of the test compounds were in the range 6.25 to 100 µg/ml. The test compound **4a**, showed promising activity towards the Gram-negative strain *E. coli* NCIM 2065 with an MIC of 6.25 µg/ml compared to the standard drugs methicillin and amoxicillin (MIC of 12.5 µg/ml). In case of *S. aureus* NCIM 5021, the test compound **4a** (MIC of 12.5 µg/ml), **2a** and **3a** (MIC of 25 µg/ml) were found to have significant activity when compared to methicillin and amoxicillin (MIC of 25 µg/ml). Amoxicillin showed slightly higher activity against *S. aureus* NCIM 5022 with an MIC of 12.5 µg/ml, while, the test compounds failed to show any prominent activity towards the same. The test compounds were not able to show any significant activity towards *B. subtilis* NCIM 2063 and *P. aeruginosa* NCIM 2200. It is clearly evident from

above result that compound possesing hydroxypropyl side chain attached to third position of the thiazolopyrimidine ring (in **4a**) increases the antibacterial activity against *E. coli* NCIM 2065 and *S. aureus* NCIM 5021. It is also evident that *N*,*N*-diethyl acetamide side chain at position three of the thiazolopyrimidine ring (in **3a)** increase the antibacterial activity against *S. aureus* NCIM 5021 and *B. subtilis* NCIM 2063. The 2,4-dihydroxy phenyl ring at seventh position of the thiazolopyrimidine ring (in **3a** and **4a)**, is crucial for imparting significant antibacterial activity. The MIC values in µg/ml of the synthesized molecules and standard drugs are listed in Table 6.

Table 6. Determination of the minimum inhibitory concentration of the synthesized molecules and standard drugs against selected strains of microorganisms.

Compound	Minimum inhibitory concentration (µg/ml)[a]				
	S.a 5021[b]	*S.a* 5022[c]	*B.s* 2063[d]	*E.c* 2065[e]	*P.a* 2200[f]
2a	25	100	100	>100	>100
3a	25	100	50	100	>100
4a	12.5	>100	>100	6.25	>100
4b	50	100	>100	>100	>100
methicillin	25	25	50	12.5	12.5
amoxicillin	25	12.5	12.5	12.5	12.5

[a]Average of three independent determinants. [b]*S.a.*: *Staphylococcus aureus* (NCIM 5021); [c]*S.a.*: *Staphylococcus aureus* (NCIM 5022); [d]*B.s.*: *Bacillus subtilis* (NCIM2063); [e]*E.c.*: *Escherichia coli* (NCIM 2065); [f]*P.a.*: *Pseudomonas aeruginosa* (NCIM 2200).

CONCLUSION

In the present investigation, novel 3,7-disubstituted-[1,3]thiazolo[4,5-*d*]pyrimidin-2(3*H*)-ones derivatives (**2a**, **3a**, **4a** and **4b**) were synthesized and characterized. The antibacterial studies exhibited satisfactory results (12-15 mm zone of inhibition) when compared with known antibacterial agents like methicillin and amoxicillin (13-24 and 20-32 mm, respectively). The test compound **3a** showed promising inhibitory activity against *S. aureus* NCIM 5021, *S. aureus* NCIM 5022, *B. subtilis* NCIM 2063 and *E. coli* NCIM 2065. In the MIC studies, compound **4a** exhibited maximum inhibitory activity against *E. coli* NCIM 2065 and *S. aureus* NCIM 5021 with MIC values of 6.25 and 12.5 µg/ml, respectively. The docking studies of synthesized molecules were performed within the active site of GyrB (PDB ID: 1AJ6) and ParE (PDB ID: 1S14). The Glide scores of the molecules were in the range -4.298 to -6.602 kcal mol^{-1} compared to the standard drug novobiocin (-6.046 kcal mol^{-1}) towards GyrB. In case of ParE, the Glide score range was -4.802 to -5.670 kcal mol^{-1} compared to novobiocin (-4.954 kcal mol^{-1}). The synthesized compounds also exhibited hydrogen bonding interactions with the key amino acid residues of active site. The QikProp descriptors and properties indicated that all these synthesized compounds are having safe ADMET parameters. Taking into consideration the structural features of the synthesized compounds, [1,3]thiazolo[4,5-*d*]pyrimidin-2(3*H*)-one scaffold can be used to develop newer antibacterial agents.

REFERENCES

Azam, M.A., Thathan, J., & Jubie, S. (2015). Dual targeting DNA gyrase B (GyrB) and topoisomerase IV (ParE) inhibitors: A review. *Biorganic Chemistry*, 62, 41-63.

Barry, A.L.J. (1999). The Antimicrobial Susceptibility Test, Principle and Practices. Lea & Febiger, *Medical*, 4, 180.

Collin, F., Karkare, S., & Maxwell, A. (2011). Exploiting bacterial DNA gyrase as a drug target: current state and perspectives. *Applied Microbiology and Biotechnology*, 92, 479-497.

Desai, K., Patel, R., & Chikhalia, K. (2006). Synthesis of pyrimidine based thiazolidinones and azetidinones: Antimicrobial and antitubercular agents. *International Journal of Industrial Chemistry*. 45, 773-778.

Friesner, R.A., Murphy, R.B., Repasky, M.P., Frye, L.L., Greenwood, J.R., Halgren, T.A., Sanschagrin, P.C., & Mainz, D.T. (2006). Docking and scoring incorporating a model of hydrophobic enclosure for protein-ligand complexes. *Journal of Medicinal Chemistry*, 49, 6177-6196.

Gellert, M., O'Dea, M.H., Itoh, T., & Tomizawa J. (1976). Novobiocin and coumermycin inhibit DNA supercoiling catalyzed by DNA gyrase. *Proceedings of the National Academy of Sciences of the United States of America*, 73, 4474-4478.

Greenwood, J.R., Calkins, D., Sullivan, A.P., & Shelley, J.C. (2010). Towards the comprehensive, rapid and accurate prediction of the favorable tautomeric states of drug-like molecules in aqueous solution. *Journal of Computer Aided Molecular Design*, 24, 591-604.

Heide, L. (2009). The aminocoumarins: biosynthesis and biology. *Nature Product Reports*. 26, 1241-1250.

Hooper, D.C. (2001). Emerging mechanisms of fluoroquinolone resistance. *Emerging Infectious Diseases*, 7, 337.

Jacobson, M.P., Pincus, D.L., Rapp, C.S., Day, T.J., Honig, B., Shaw, D.E., & Friesner, R.A. (2004). A Hierarchical approach to all-atom protein loop prediction. *Proteins: Structure Function and Bioinformatics*, 55, 351-367.

Laponogov, I., Sohi, M.K., Veselkov, D.A., Pan, X.S., Sawhney, R., Thompson, A.W., McAuley, K.E., Fisher, L.M., & Sanderson, M.R. (2010). Structural insight into the quinolone-DNA cleavage complex of type IIA topoisomerases. *Nature Structural and Molecular Biology*, 16, 667-669.

Maxwell, A. (1997). DNA Gyrase as a drug target. *Trends in Microbiology*, 5, 102-109.

Oblak, M., Kotnik, M., & Solmajer, T. (2007). Discovery and development of ATPase inhibitors of DNA gyrase as antibacterial agents. *Current Medicinal Chemistry*, 14, 2033.

Ohtake, Y. C. (2008). U.S. Patent Application No. 2008/0076760 A1. Washington, DC: U.S. Patent and Trademark Office.

Ottana, R., Maccari, R., Barreca, M.L., Bruno, G., Rotondo, A., Rossi, A., Chiricosta, G., Paola, R.D., Sautebin, L., Cuzzocrea, S., & Vigorita, M.G. (2005). 5-Arylidene-2-imino-4-thiazolidinones: design and synthesis of novel anti-inflammatory agents. *Bioorganic Medicinal Chemistry*, 13, 4243-4253.

Pattan, S., Kedar, M., Pattan, J., Dengale, S., Sanap, M., Gharate, U., Shinde, P., & Kadam, S. (2012). Synthesis and evaluation of some novel 2, 4-thiazolidinedione derivatives for antibacterial, antitubercular and antidiabetic activities. *Indian Journal of Chemistry- Section B*, 51, 1421-1425.

Sastry, G.M., Adzhigirey, M., Day, T., Annabhimoju, R., & Sherman, W. (2013). Protein and ligand preparation: parameters, protocols and influence on virtual screening enrichments. *Journal of Computer Aided Molecular Design*, 27, 221-234.

Shivakumar, D., Williams, J., Wu, Y., Damm, W., Shelley, J., & Sherman, W. (2010). Prediction of absolute solvation free energies using molecular dynamics free energy perturbation and the OPLS force field. *Journal of Chemical Theory and Computation*, 6, 1509-1519.

Sissi, C., & Palumbo, M. (2010). In front of and behind the replication fork: bacterial type IIA topoisomerases. *Cellular and Molecular Life Sciences*, 67, 2001-2024.

Tari, L.W., Trzoss, M., Bensen, D.C., Li, X., Chen, Z., Lam, T., Zhang, J., Creighton, C.J., Cunningham, M.L., Kwan, B., Stidham, M., Shaw, K.J., Lightstone, F.C., Wong, S.E., Nguyen, T.B., Nix, J., & Finn, J. (2013). Pyrrolopyrimidine inhibitors of DNA gyrase B (GyrB) and topoisomerase IV (ParE). Part I: Structure guided discovery and optimization of dual targeting agents with potent, broad-spectrum enzymatic activity. *Bioorganic Medicinal Chemistry Letters*, 23, 1529-1536.

Walsh, C. (2003). Antibiotics: Actions, origins, resistance, Vol. 1, *Protein Science*.

Walsh, T.J., Auger, F., Tatem, B.A., Hansen, S.L., & Standiford, H.C. (1986). Novobiocin and rifampicin in combination against methicillin-resistant *Staphylococcus aureus*: an *in-vitro* comparison with vancomycin plus rifampicin. *Journal of Antimicrobial Chemotherapy*, 17, 75-82.

Walsh, T.J., Hansen, S.L., Tatem, B.A., Auger, F., & Standiford, H.C. (1985). Activity of novobiocin against methicillin-resistant *Staphylococcus aureus*. *Journal of Antimicrobial Chemotherapy*, 15, 435-440.